Vision Research 118 (2016) 119–131

Contents lists available at ScienceDirect

Vision Research

journal homepage: www.elsevier.com/locate/visres

Oculomotor behavior of blind patients seeing with a subretinal visual implant

Ziad M. Hafed [a,*], Katarina Stingl [b,*], Karl-Ulrich Bartz-Schmidt [b], Florian Gekeler [c], Eberhart Zrenner [a,b]

[a] Werner Reichardt Centre for Integrative Neuroscience, Otfried-Mueller Strasse 25, Tuebingen 72076, Germany
[b] Center for Ophthalmology, Institute for Ophthalmic Research, University of Tuebingen, Schleichstrasse 12-16, Tuebingen 72076, Germany
[c] Augenklinik Katharinenhospital, Klinikum Stuttgart, Kriegsbergstrasse 60, Stuttgart 70174, Germany

ARTICLE INFO

Article history:
Received 21 August 2014
Received in revised form 31 March 2015
Available online 20 April 2015

Keywords:
Subretinal electronic implant
Retina Implant Alpha IMS
Gaze fixation
Microsaccades
Fixational eye movements
Retinitis pigmentosa

ABSTRACT

Electronic implants are able to restore some visual function in blind patients with hereditary retinal degenerations. Subretinal visual implants, such as the CE-approved Retina Implant Alpha IMS (Retina Implant AG, Reutlingen, Germany), sense light through the eye's optics and subsequently stimulate retinal bipolar cells via ~1500 independent pixels to project visual signals to the brain. Because these devices are directly implanted beneath the fovea, they potentially harness the full benefit of eye movements to scan scenes and fixate objects. However, so far, the oculomotor behavior of patients using subretinal implants has not been characterized. Here, we tracked eye movements in two blind patients seeing with a subretinal implant, and we compared them to those of three healthy controls. We presented bright geometric shapes on a dark background, and we asked the patients to report seeing them or not. We found that once the patients visually localized the shapes, they fixated well and exhibited classic oculomotor fixational patterns, including the generation of microsaccades and ocular drifts. Further, we found that a reduced frequency of saccades and microsaccades was correlated with loss of visibility. Last, but not least, gaze location corresponded to the location of the stimulus, and shape and size aspects of the viewed stimulus were reflected by the direction and size of saccades. Our results pave the way for future use of eye tracking in subretinal implant patients, not only to understand their oculomotor behavior, but also to design oculomotor training strategies that can help improve their quality of life.

1. Introduction

Because of the tremendous reliance of humans on the sense of vision, vision loss constitutes a significant disability with large implications on quality of life. Neurodegenerative diseases of the outer retina, such as retinitis pigmentosa, are particularly problematic because they lead to blindness over several years, or even decades, without an established therapy. These progressive and hereditary diseases are characterized by degeneration of the rods and cones, whereas inner retinal circuitry and afferent visual pathways remain mostly functional.

Attempts at improving the condition of visually-impaired patients by visual neuroprosthetics go far back (reviewed by Zrenner, 2002, 2013), and there are many research groups working in the field. However, only two retinal visual implant devices are currently approved for use in humans: the subretinal Retina Implant Alpha IMS (Retina Implant AG, Reutlingen, Germany) (Stingl, Bartz-Schmidt, Gekeler et al., 2013; Stingl, Bartz-Schmidt, Besch et al., 2013; Zrenner, 2002, 2013; Zrenner et al., 2011), and the epiretinal implant Argus II (Second Sight Medical Products, Inc., Sylmar, California) (Humayun et al., 2012). Even though both devices stimulate the inner retina, they represent two qualitatively very different approaches to visual prosthetics.

In the Argus II epiretinal implant (Humayun et al., 2012), a head-mounted camera captures the scene, and images are decoded for stimulation of retinal ganglion cells and their axons at the retinal output site. This is done by an epiretinally fixed 60-electrode array. On the other hand, the Retina Implant Alpha IMS (Stingl, Bartz-Schmidt, Gekeler et al., 2013; Stingl, Bartz-Schmidt, Besch et al., 2013; Zrenner et al., 2011) simultaneously captures the image and stimulates bipolar cells at the retinal input site using a ~1500 pixel microphotodiode-electrode array implanted under the retina (Fig. 1A). Essentially, the Retina Implant Alpha IMS replaces photoreceptor function with an electronic array of light-sensitive photodetectors. These light-sensitive elements are connected to amplifiers and stimulating electrodes, such that when

* Corresponding authors.
E-mail addresses: ziad.m.hafed@cin.uni-tuebingen.de (Z.M. Hafed), katarina.stingl@med.uni-tuebingen.de (K. Stingl).

http://dx.doi.org/10.1016/j.visres.2015.04.006
0042-6989/

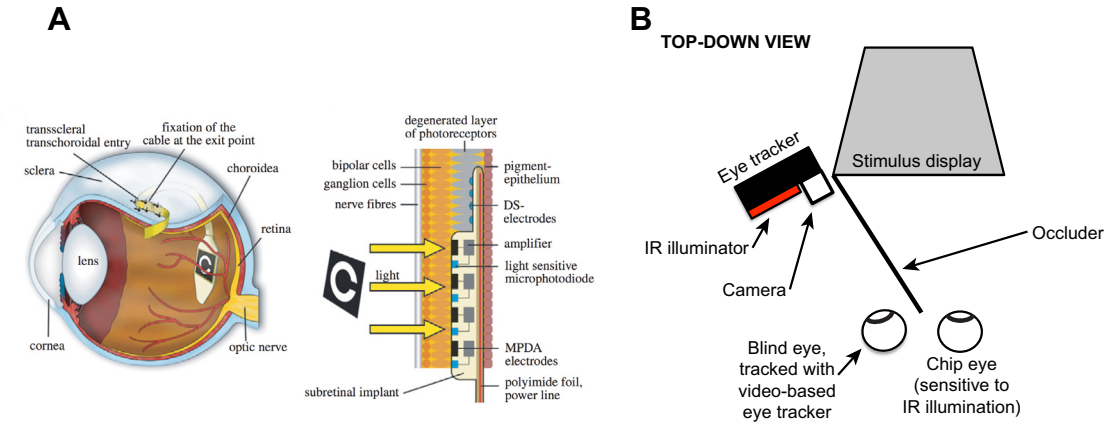

Fig. 1. Subretinal electronic implant and laboratory setup for eye tracking in the current study. (A) A microchip (the microphotodiode-electrode array) is implanted subretinally under the central visual field representation of the retina (left panel). The chip is tethered to a power supply cable that is threaded out of the eye and on towards a subdermal coil behind the ear. The right panel shows a side view schematic of the retina with the chip implanted as a replacement for degenerated photoreceptors. Each "pixel" of the chip consists of a canonical circuit consisting of a photodetector, amplifier, and electrical stimulator. Light activates the photodiodes, and the connected electrodes stimulate the retina. Image adapted from Zrenner et al. (2011). (B) In the present study, we tracked the non-implanted eye using a standard video-based eye tracker. An occluder was placed in front of the subject such that the non-implanted eye was tracked while the implanted eye viewed the stimulus. Since the photodiodes in the implant are sensitive to infrared illumination, the current setup allowed the subjects to view the stimuli without their implant being flooded with the infrared light coming from the eye tracking system (see Section 2).

light hits the photodetectors, it is converted into electrically graded potentials that stimulate bipolar cells (Eickenscheidt et al., 2012). By involving even the bipolar cells, the Retina Implant Alpha IMS harnesses the full signal processing potential of the inner retina, which remains intact for many decades in most retinitis pigmentosa patients.

A further advantage of subretinal implants is that eye movements allow moving the captured images over the stimulated retina, much like they do in natural vision. Thus, the implant allows patients to use their natural oculomotor behavior to scan scenes and fixate objects. This is important because eye movements are an integral component of vision. At the macro-scale, they allow foveating new objects for closer inspection, and at the micro-scale, eye movements during fixation are thought to optimize eye position (Hafed, Goffart, & Krauzlis, 2009; Kagan & Hafed, 2013; Ko, Poletti, & Rucci, 2010; Poletti, Listorti, & Rucci, 2013), refresh retinal images from fading (Coppola & Purves, 1996; Riggs et al., 1953), and even modulate visual processing in the brain (Hafed, 2013; Hafed & Krauzlis, 2010; Kagan, Gur, & Snodderly, 2008; Leopold & Logothetis, 1998). In visual prosthetics with head-mounted cameras, such as the Argus II, patients have to learn to use relatively coarse head movements for visual search instead.

The Retina Implant Alpha IMS can convert the state of blindness (defined in the ophthalmic sense as the absence of light source localization) into that of low or very low vision, and it does so by mediating a central visual field of ~10–15° of visual angle with a limited spatial resolution; the best visual acuity measured by standardized tests so far was 20/546, which is the highest published resolution for visual neuroprosthetics so far (Stingl, Bartz-Schmidt, Gekeler et al., 2013; Stingl, Bartz-Schmidt, Besch et al., 2013; Zrenner et al., 2011). However, to date, there have been no systematic attempts at investigating the role of eye movements in subretinal implant patients. In this study, we characterized such role in two patients. We were particularly interested in understanding potential oculomotor factors that may induce onsets or offsets of percepts. We found that patients fixated well when they perceived stimuli through the implants, and that their fixational eye movements were qualitatively similar to controls, even with very little training. More significantly, we noticed important associations and dissociations between visibility reports and oculomotor characteristics, suggesting that eye tracking can be an extremely useful objective measure for evaluating patient success in retinal implants, as well as a promising tool for training these patients on visuomotor coordination.

2. Methods

2.1. Subjects

We tracked eye movements in two male patients with a subretinal visual implant (Retinal Implant AG, Reutlingen, Germany). Both patients were blind (their visual function exhibited light perception without correct light source localization) due to end-stage retinitis pigmentosa, and they received the implant in only one eye (right eye for TU-09 and left eye for TU-21). The implant covered the central visual field in both patients, although it was slightly biased to the nasal side in patient TU-21. Furthermore, the image was perceived in gray levels (no color vision), similar to older black-and-white television sets, since all ~1500 microphotodiodes of the implant have equal light sensitivity, and since the implant stimulates bipolar cells equally regardless of whether these cells had received rod or cone signals earlier.

The perceived image was also slightly flickering because the implant stimulates the retina at regular intervals (usually 5 Hz, adjustable from 1 Hz to 20 Hz); at a given frequency, the implant captures light and stimulates the retina with a 1 ms pulse (individually adjustable up to 4 ms). We tested patient TU-21 in one session with his implant operating at 5 Hz. We tested patient TU-09 in two separate sessions, using 2 Hz in the first session and 5 Hz in the second. Even though the implant itself can run at higher frequencies, we strived to run our patients with the lowest possible frequencies providing usable percepts. We did so in order to minimize the amount of electrical charge transmitted to the retina, which can potentially cause tissue damage.

To compare patient performance to that of healthy control subjects, we also ran 3 controls on the same tasks performed by the patients, as well as additional control variants of them (see below). One of the controls was an author (ZH), whereas two others (FC8 and CH) were naïve to the purposes of the study.

Our experiments were approved by the local ethics committee at Tuebingen University, and were in accordance with the Code of Ethics of the World Medical Association (Declaration of Helsinki) for experiments involving humans.

2.2. Laboratory setup

The laboratory setup was similar to that described recently (Hafed, 2013). Briefly, subjects sat in front of a computer monitor displaying stimuli at 85 Hz refresh rate and 41 pixels/deg spatial resolution. A subject's head was stabilized in front of the display using a chin- and forehead-rest. However, we did not fix the patients' heads as strictly as we normally do with control subjects (Hafed, 2013), in order to minimize any potential discomfort to them.

We employed a non-invasive video-based eye tracker (EyeLink 1000, SR Research, Ontario, Canada). The eye tracker was desktop mounted, and it sampled eye position at 1 kHz. The eye tracker illuminates the eye with a fairly strong source of infrared (IR) radiation. Normally, this dramatically increases the dynamic range of eye tracker images because electronic photodetectors (such as CCD or CMOS image sensors) are sensitive to IR radiation ranges. Thus, an IR illuminator allows the eye tracker to detect the pupil and corneal reflection with a properly illuminated image for its camera, while at the same time minimizing discomfort to subjects who would not see the illuminator's radiation. However, since the microphotodiodes of the subretinal implant are also sensitive to IR radiation, such a setup constituted a major challenge; the IR illuminator of the eye tracker flooded our patients' field of view with bright "light" perception.

In order to avoid this issue, we adjusted the geometry of the laboratory as shown in Fig. 1B. We placed an occluder in front of each patient such that only the implanted eye viewed the stimulus display, while the other (blind) eye was occluded from the display (but in direct view of the eye tracker camera and illuminator). Thus, the eye tracker could illuminate the tracked eye and measure it without flooding the chip eye as this second eye viewed the stimulus display. In other words, we exploited conjugacy of eye movements to track the blind eye while the implanted eye was viewing the stimulus. As seen often in acquired blindness, for patient TU-09, the non-chip eye (i.e. the non-seeing eye) was slightly divergently strabismic (Fig. 1B), but it did move conjugately with the other eye (as assessed with a standard ophthalmic test).

Note that the above geometry posed some challenges. First, the geometry of eye tracking was not as optimal as with the camera being aimed from directly in front of the subject. This may have caused some distortions in calibration (see Section 3), but we were nonetheless still able to obtain reliable data. Second, measurement of the non-chip eye restricted us to measuring eye movements of the seeing eye only indirectly. It cannot be fully excluded that some components of our measured eye movements (e.g. a fraction of ocular drift during fixation) were only specific to the blind eye that we were tracking. Third, for some extreme eye rotations, the geometry of the eye tracker camera meant that we sometimes lost the eye image (e.g. due to occlusion from eye lids, which was sometimes exacerbated when the patients squinted), meaning that we had a slightly lower range of possible angular eye positions than with the camera being directly in front of the subjects. In this case, we attempted to display stimuli only near screen center in order to still obtain useful eye tracking data.

We also took additional measures to ensure that the above technical challenges were handled adequately. Specifically, and in order to compare our patients to controls with as similar a set of conditions as possible, we ran our controls with exactly the same setup as in Fig. 1B.

2.3. Stimuli and procedures

Sitting in a dark room, subjects viewed bright geometric shapes presented on a dark background. The shapes had luminances of either 97 cd/m^2 or 28 cd/m^2. The choice of luminance was made to avoid discomfort to our patients from excessively bright stimuli.

Each patient session consisted of several hours of tests, separated by sufficient breaks. For each test, the patient repeated 10–30 trials of a task (3 variants, see below) consisting of a specific stimulus presentation. In each of the test variants, the patient first pressed a button to start a trial. After 700–3000 ms, a stimulus appeared at one possible screen location (specified below). The observer's task was to search for the stimulus and then press and hold a button for as long as he could see it. When he no longer saw the stimulus (i.e. he lost the percept of the stimulus for whatever reason), the patient was to release the button. The stimulus remained on the display for 50.5 s in every trial, and the patient pressed and released the button as many times as he found or lost the stimulus, respectively.

2.3.1. Localization

A white filled circle of radius 1.22° appeared randomly at one of 9 possible locations: screen center; ±4.9° horizontally from screen center; ±4.9° vertically from screen center; or ±4.9° horizontally and ±4.9° vertically from screen center. Thus, across trials, the stimulus covered a grid of evenly spaced locations on the display, pseudorandomly shuffled across trials. This task allowed us to establish that eye movements reflect visual percepts by the implants, and to also obtain an approximate calibration of eye measurements (see below and Section 3).

2.3.2. Shapes

In order to examine scanning eye movements in our patients during shape viewing, we presented different geometric shapes, and the patients attempted to report these shapes when they saw them. A stimulus was always presented at the screen center, and it could be one of five possible geometric shapes, again presented pseudorandomly across trials. These shapes were as follows: (1) the same circle as above; (2) a square of 2.44° dimensions; (3) a horizontal rectangle (2.44 × 1.22°); (4) a half-circle of the same radius as the circle above but cut along a horizontal line such that only the bottom half was visible; (5) and, finally, an equilateral triangle pointing downward with side length 2.44°. This task allowed us to ask whether eye movement patterns could be influenced by shape, as is known to happen in the oculomotor system (Moore, 1999; Yarbus, 1967).

2.3.3. Control tasks

For controls, we ran the above tasks, as well as additional versions of them with the visual stimuli flickering at either 2 or 5 Hz. With visual flicker, a stimulus was only visible for ~12 ms in every flicker cycle. These conditions were run to simulate a possible influence of periodic electrical stimulation by the implants on our patients' eye movements.

2.3.4. Setting of implant characteristics

Contrast sensitivity and gain of the amplifiers within the chip can be adjusted to ambient luminance and contrast by the patient. Both parameters were set by each patient prior to the experiments, so that the luminance of the stimulus was visible over the dark background.

2.4. Data analysis

During stimulus presentation, the patients pressed and held a button while they had a percept of a stimulus and released it when

the percept disappeared. Across all trials, we measured the durations of button presses as our estimates of visibility durations. Note that we only considered visibility durations longer than 5 ms because the patients sometimes pressed erroneously and briefly, especially at the beginning of a session.

To study the patients' eye movements, we applied two main classes of analyses. In one class, we analyzed eye position during periods of visibility reports by the subjects, and we compared it to that obtained during periods of invisibility reports. This class of analysis was particularly useful for us in the localization task, in order to obtain an approximate calibration regime for our patients (see below and Section 3), and it was also useful in our investigation of how factors like ocular drift may have affected whether patients transitioned from periods of visibility to periods of invisibility.

For the second class of analyses, we numerically differentiated eye position to obtain eye velocity and eye acceleration estimates, as described recently (Chen & Hafed, 2013). This allowed us to detect saccades and microsaccades using velocity and acceleration criteria (Hafed et al., 2009; Krauzlis & Miles, 1996), and we also manually inspected all data to remove false alarms and add misses. Once we obtained these saccades, we analyzed their metrics, as well as their frequency and inter-movement intervals.

In all analyses, we excluded all eye movement measurements that were corrupted either by occluded pupils (leading to excessive noise in the measurements) or blinks (leading to a loss of eye data since the eyes were closed). For blinks, we also excluded an interval of 150 ms before or after each blink to avoid artifactual eye movements associated with the blink itself. All error bars we show denote standard errors of the mean.

2.4.1. Eye position calibration

For some analyses, we needed to get estimates on the sizes and other metrics of our measured eye movements. To do this, we used the localization task to obtain an approximate calibration for each of our subject's raw eye tracker measurements. We applied the following procedure. For each stimulus location, we measured the average eye position in raw eye tracker coordinates, but only when the patient reported seeing the stimulus (i.e. we assumed that the eye looked at the stimulus when the patient reported seeing the latter, an assumption that we validated in Fig. 4). Using these measurements, we then fitted a straight regression line through the eye position measurements for stimuli located along the horizontal axis of our stimulus display (i.e. we fit a straight line for the eye position measurements of the pure left stimulus, the central stimulus, and the pure right stimulus). We also fitted a straight line through eye position measurements for stimulus locations along the vertical axis of our stimulus display (i.e. the up stimulus, the central stimulus, and the down stimulus). These straight lines were approximately orthogonal to each other (see Fig. 4 and Section 3), but they were tilted relative to the screen coordinates (because of the geometry of the eye tracker camera relative to the subjects' eyes). Thus, the raw eye tracker measurements could be converted to calibrated visual angle measurements (i.e. in screen coordinates) through a simple affine rotation and scaling (Fig. 4). After we obtained the parameters of such transformation, we applied it to all eye movement data (including the diagonal stimulus locations).

In principle, one can apply more sophisticated calibration routines and improve the estimates even further despite the unusual eye tracking geometry (e.g. Stampe, 1993) used interaction terms between horizontal and vertical eye tracking measurements). However, for all of our experiments besides localization, we presented stimuli at screen center, where our simple calibration approach was still usable, and where geometrical distortions were not evident. Therefore, we elected to maintain the simplest possible calibration routine. Also, calibration of our patients would be inherently variable even with different eye tracker camera placement, because of the limited spatial resolution of their implants.

3. Results

We first measured the duration of visibility reports by the patients. We used the term "duration" in relation to the time period during which the patient saw the stimulus before an eye movement shifted this stimulus away from the visual field mediated by the implant. This term is therefore not necessarily related to the fading of percepts evoked by electrical stimulation of the retina (Perez Fornos et al., 2012), a phenomenon which is particularly strong with head-mounted camera implants in which eye-movement-induced retinal image refreshing is not possible. Patient TU-09 exhibited an average visibility duration of ~581 ± 13.63 ms s.e.m. (316 measurable visibility reports) at 2 Hz, whereas with 5 Hz, visibility durations were much longer: ~11,666 ± 1602 ms s.e.m. (43 measurable visibility reports). Patient TU-21's visibility durations, with the implant running at 5 Hz, were ~6037 ± 478 ms s.e.m. (138 measurable reports). Note that this patient's visibility durations were also very stable (i.e. with lower variance across measurements than in patient TU-09 with 5 Hz).

We hypothesized that oculomotor patterns contribute to percept quality. After all, the patients were looking at the world through a "window" of visibility achieved via their implants, and if they simply moved their eyes such that the image sensor of their implant covered an area without a stimulus, they would be expected to lose visibility. If this is the case, then this has strong implications on oculomotor training strategies for these patients in order to improve their performance with their implants. In what follows, we show how eye tracking in subretinal implant patients can provide an objective measure of implant performance, as well as an indication of the potential role of eye movements in maintaining or modulating stimulus visibility.

3.1. Eye fixations reflected the patients' percepts

We first asked whether eye movements would behave differently when patients reported seeing a stimulus versus when they reported not seeing it. We plotted raw eye tracker data during sample trials and marked on these trials whether the patients had seen the presented stimulus or not (Fig. 2A and B for patient TU-21 during searching of a circle of 1.22° radius, and Fig. 2C for patient TU-09 performing the same task). The blue curves show raw "horizontal" eye tracker measurements as a function of time, and the red curves show raw "vertical" eye tracker measurements. In both figures, we obtained the eye position scale bars based on a subsequent calibration procedure (Section 2and Fig. 4). Above each trial's eye position data, we indicated the intervals in which the patient reported seeing the stimulus ("Visible") and the intervals in which he reported not seeing it ("Not visible").

Eye movement patterns during periods of visibility were dramatically different from patterns during periods of invisibility. For example, in Fig. 2A, there was a transition from no visibility to visibility at ~11.7 s after trial onset (first vertical black line). Around this transition, there was a marked change in eye movements. Without visibility, eye movements were large and scanning (black arrows); the patient was actively searching for any light source. During visibility, much more stable fixation was observed. In the trial of Fig. 2B, a similar pattern could also be seen. Interestingly, this trial also showed a second visibility transition, but this time one with the opposite polarity: the patient transitioned from a period of several seconds of visibility to a period of invisibility. Again, his fixation became less stable after he lost the percept (black arrow in Fig. 2B). In this case, after losing a prior

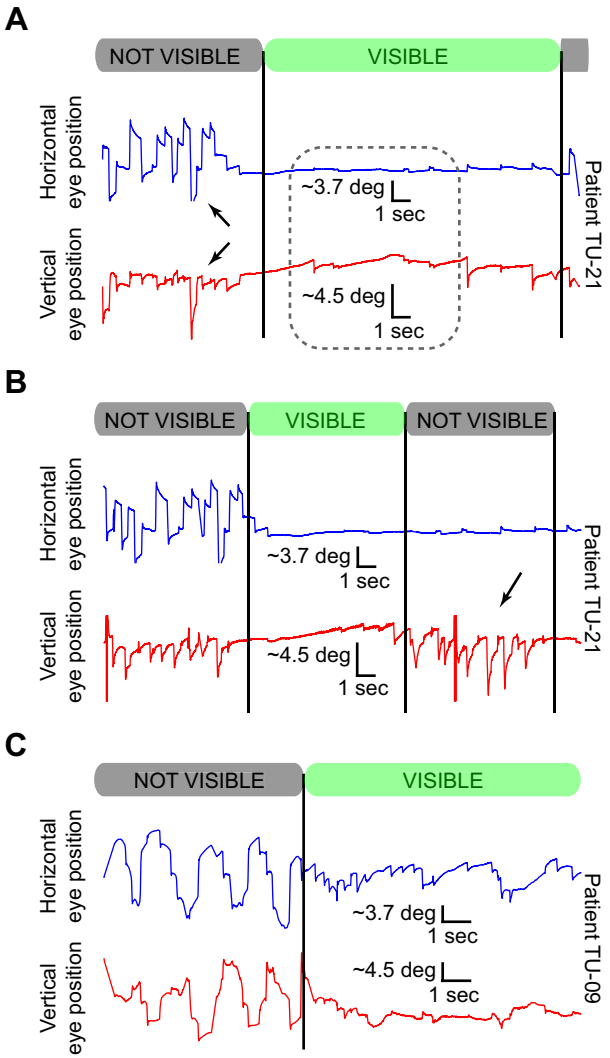

Fig. 2. Eye movements of blind patients using the subretinal implant strongly reflected their percepts of a stimulus. (A, B) Raw eye tracker traces from two sample trials from patient TU-21. Blue traces show the "horizontal" component of the raw tracker measurements, and red traces show the "vertical" component. Above the traces, we show a timeline of the subjective report of the patient on whether he saw the stimulus or not. The eye position scale bars were obtained based on a calibration procedure described in Fig. 4 and the text. Note that because these traces are raw, higher "vertical" measurement values indicate downward eye movements (see Fig. 4). As can be seen, eye movements were large and frequent without a percept but fixation became stable during a percept. The black arrows show examples of large scanning eye movements when the patient could not see the stimulus. The dashed square in A highlights a period of stable fixation, which is presented in greater detail in Fig. 3. (C) A similar trial to those in A, B but from patient TU-09. Very similar observations were made. The patient exhibited more stable eye position when he saw the stimulus compared to when he could not see it. However, note that this patient exhibited nystagmus during fixation, resulting in frequent corrective fast phases (particularly visible in horizontal eye position). Supplementary Movie S1 shows additional example eye position trajectories in real-time, demonstrating the marked change in oculomotor behavior of our patients with and without a stimulus percept.

percept, the patient attempted to maintain his horizontal position at the remembered stimulus location but was scanning with large vertical saccades to try to find the stimulus once again (black arrow in Fig. 2B). Finally, Fig. 2C shows data from the second patient (TU-09) showing a similar pattern to TU-21 (compare to Fig. 2A), although this patient exhibited marked nystagmus while fixating the visible stimulus. It is not entirely clear to us whether this nystagmus was also present in the implanted eye that was viewing the stimulus, or whether it was specific to the tracked blind eye. Interestingly, some control subjects do sometimes show a microform of nystagmus when fixating, especially when the subjects are fatigued.

Thus, during periods of visibility, fixation in both patients became more constrained than without visibility. However, even during this constrained fixation, the patients still made smaller eye movements that are known in controls to be influential in vision. Specifically, besides the nystagmus in Fig. 2C, we observed fixational traces in both of our patients that looked similar to those of controls: the patients generated ocular drifts and fixational saccades when they were actively fixating a stimulus. To illustrate this, we plotted in Fig. 3A a portion of a fixational trace by one of our patients when he reported seeing the stimulus (this is the portion that is highlighted by a dashed square in Fig. 2A). In Fig. 3B, we plotted a similar portion of fixation but now from one of our control subjects. As can be seen, the patient exhibited periods of slow ocular drifts that were occasionally interspersed with small fixational saccades (examples indicated with black arrows). Moreover, the range of variability of eye position during fixation was similar to the range of variability that the control subject exhibited (compare to Fig. 3B). Interestingly, some of the fixational saccades that the patient made came in pairs of largely oppositely directed movements (Fig. 3A, and a highlighted example from this trial in Fig. 3C). These pairs of small, opposing fixational saccades are sometimes referred to as "square waves" (Abadi, Scallan, & Clement, 2000; Feldon & Langston, 1977; Hafed & Clark, 2002), and they have been previously related to factors beyond just oculomotor control, like visual attention (Hafed & Clark, 2002; Pastukhov & Braun, 2010; Pastukhov et al., 2012). In our patients, these square waves were similar to those exhibited by controls (compare to Fig. 3D), and their presence in the patients suggests that their roles in visuomotor functions may still hold in these patients as well.

Thus, eye movements in our patients were qualitatively similar to those of the control subjects, and they therefore provided an objective measure of "seeing" stimuli even if the patients themselves were sometimes hesitant or uncertain about either stimulus location or identity. More importantly, we were now confident that we could use a "localization" task (see Section 2) to calibrate the eye tracker and do further analyses on eye movement metrics with and without visual percepts.

3.2. Eye movements reliably reflected stimulus location

Having established that fixation became more stable during periods of visibility reports, we next asked whether such stable fixation was meaningfully correlated with stimulus location. For each time interval in which a patient reported seeing a stimulus, we calculated the average eye position during fixation of the stimulus. Fig. 4A (left panel) shows a scatter of such averages across all periods of visibility from patient TU-21 for 8 different (color-coded) stimulus locations. Each color-coded point represents the average eye position across all visibility reports for a given stimulus location, and the data is presented in raw eye tracker measurement coordinates. The horizontal/vertical error bars around each data point indicate s.e.m. The eye fixation position (in raw eye tracker coordinates) differed clearly among the various physical stimulus locations. Thus, eye movements reliably reflected stimulus location.

We used the above observations to obtain approximate "calibrated" resolution estimates from our patient eye tracking data. As described in Section 2, we first fitted a straight regression line through the data points in the figure that covered the horizontal axis (Fig. 4A, left panel, dashed line best fitting the red, blue, and green measurements). We then fitted a straight line through the data points that covered the vertical axis (second dashed line best

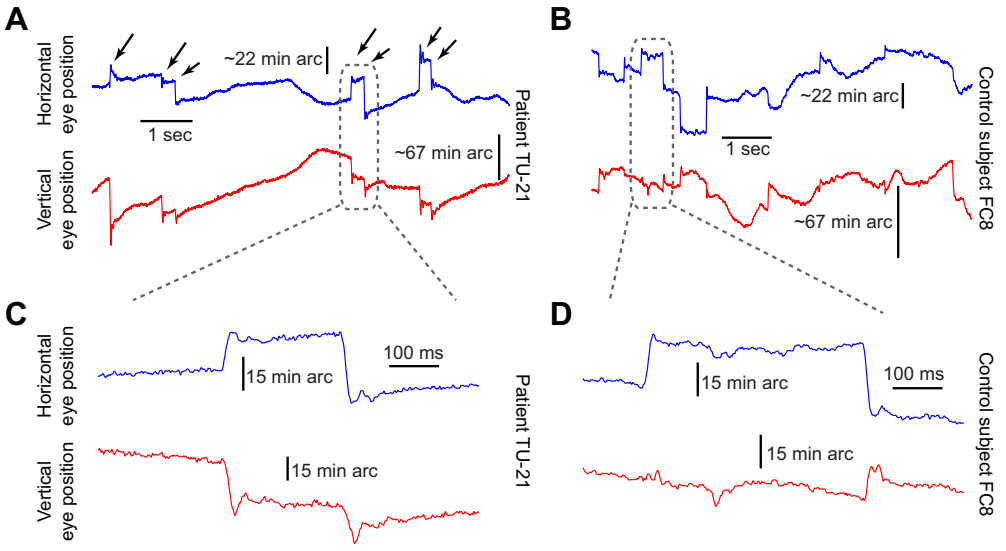

Fig. 3. Similarity of fixational eye movements in patients and controls. (A) A magnified representation of the stable fixation interval of Fig. 2A during a visibility report by patient TU-21. When the patient saw the stimulus, classic fixational drifts and fixational microsaccades were observed. The arrows highlight the microsaccades that occurred in the shown interval. (B) Data from control subject FC8 during a similar fixation interval. The ranges of variability in this subject's eye position, as well as the sizes of fixational saccades, are qualitatively similar to those of the patient. (C, D) Examples of "square-wave" microsaccades from the patient (C) and the control subject (D).

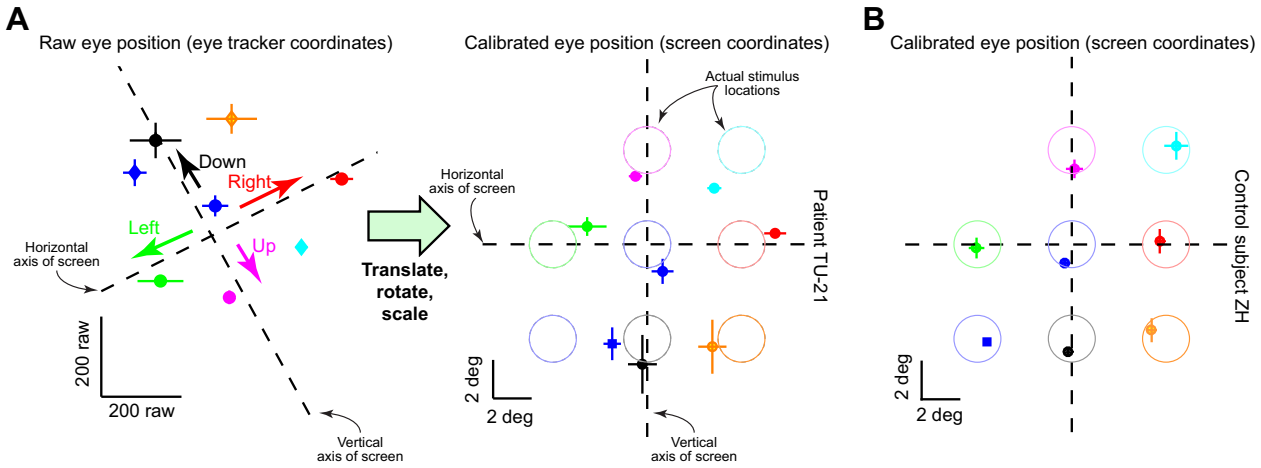

Fig. 4. Eye movements reflected stimulus location. (A) The left panel shows raw eye tracker measurements when the patient looked at a stimulus at a specific location. Each dot shows average eye position during seeing the stimulus in a particular location, and the horizontal/vertical error bars around each dot denote s.e.m. The different colored dots indicate different stimulus locations (e.g. red was when the stimulus was to the right of screen center, and magenta was when the stimulus was above screen center). The dashed lines indicate the approximate horizontal and vertical axes of our stimulus display (they are tilted because they are shown in raw camera rather than screen coordinates). As can be seen, eye position was related to stimulus position, allowing us an approximate calibration. In the right panel, we show the same data after applying the calibration routine described in the text. Now, the horizontal and vertical axes of the stimulus display coordinates have been translated and rotated to their proper orientations, and screen center is at the intersection of the two lines. The faint colored circles (like the cyan and magenta ones highlighted with arrows in the figure) are the actual stimulus locations used. As can be seen, eye position reflected stimulus location well, although there were some geometric distortions, particularly in the left visual field due to eye tracking geometry and squinting by the patient. (B) The result of applying the same procedure to a control subject's data.

fitting the magenta, blue, and black measurements). The intersection of these two lines was taken as the origin (representing screen center) and the angle of these axes relative to horizontal or vertical defined the "tilt" of the raw measurements relative to the true screen coordinates. In the patient shown in Fig. 4A (left panel), the horizontal axis tilt was 26.7° from horizontal and the vertical axis tilt was 28.7° from vertical. We next applied a simple affine rotation based on the average tilt of the two axes in order to "calibrate" eye position. Finally, we scaled horizontal and vertical measurements after the affine rotation by a resolution term that we obtained based on horizontal and vertical stimulus position relative to screen center. Specifically, for horizontal scaling, we took the average of the right (red circle) and left (green circle) eye position measurements relative to the eye position measurement for screen center (blue circle). We then scaled the raw measurements by the ratio of this average "rotation from straight ahead" to the true target eccentricity of 4.9° from screen center. We did the same for vertical scaling, in which we measured the raw distance between the vertical positions (magenta and black) from screen center (blue). For the patient shown in Fig. 4A, the horizontal scaling was 1.13 arcmin/raw eye tracker measurement, and the vertical scaling was −1.36 arcmin/raw tracker measurements. The values for the other patient (TU-09) were 0.912 arcmin/raw and −1.176 arcmin/raw for horizontal and vertical eye position, respectively. These measurements were similar in both patients, which is expected since the eye tracker camera was at a fixed distance from

the head-fixation device that we used across the different experiments (the only remaining sources of variation would likely be individual differences in the subjects' eyes).

After applying the above procedures, we obtained the data of Fig. 4A (right panel). Here, each stimulus location (and size) is shown in a faint color corresponding to the related eye position measurement obtained when the patient was looking at this location. The eye was very close to the true corresponding target location, except for the lower-left diagonal target location (blue square) for which some geometrical distortion in the eye tracker images occurred (causing miscalibration). Part of this distortion was also due to the fact that the patient squinted when looking in that direction. We also did not have sufficient measurements from this patient for the upper-left diagonal target location, and that is why this location is not shown in the figure.

To further establish that the above procedure gave us usable calibration estimates of eye data, we also ran control subjects under the same laboratory conditions. Fig. 4B demonstrates the results we obtained from one such subject. As can be seen, our calibration procedure reliably recovered this subject's eye positions across the different stimulus locations. More importantly, because this subject was able to see the stimulus and fixate it, his results support the conclusion that the patients' eye positions when they reported visibility did indeed reflect stimulus location, suggesting that the patients fixated the stimuli.

Thus, given the above analyses, we were now able to obtain estimates of the "resolution" of our eye tracker measurements in all of our control subjects and patients. This allowed us to assess eye movement metrics; we could now assess whether small saccades (even in the microsaccade amplitude range) occurred during fixation. We could also analyze oculomotor factors potentially contributing to gaining or losing visibility.

3.3. Saccade and microsaccade characteristics were similar to those of controls

We detected all saccadic events and found that saccades during visibility reports were significantly smaller than without visibility. Fig. 5A shows the main sequence relationship relating saccade amplitude to peak eye velocity from each patient individually, as well as from our three control subjects. Both patients showed saccades that fell on a main sequence relationship, similar to our controls (Zuber, Stark, & Cook, 1965). Moreover, in both patients, there was a smaller size of eye movements while fixating the object during stimulus visibility (red, left two panels) than when it was invisible and they were searching for it (blue, left two panels) (Fig. 5B). Specifically, saccades in patient TU-09 had an average amplitude of 2.37° during stimulus visibility, which was significantly smaller than 5.37° during periods of invisibility (*t*-test, $p < 2e{-}27$). Similarly, in patient TU-21, the saccades were 1.58° vs. 5.14° during periods of visibility vs. invisibility, respectively ($p < 4e{-}42$).

The fact that saccades were smaller during periods of visibility in both patients is an indication of a level of fixational stability, which is consistent with our earlier analyses of Figs. 2 and 3. Moreover, we found that the patients made small saccades, within the range of so-called microsaccades (typically less than 1° in amplitude). Finally, note that patient TU-09 exhibited somewhat more overlap in saccade sizes between percept and no percept than patient TU-21. This is likely due to the fact that this patient exhibited significant nystagmus during periods of stimulus visibility, resulting in more corrective fast phases that were larger than microsaccades (Fig. 2C).

Fig. 5 also shows an indication of the level of fixational stability that our control subjects exhibited when they viewed the same stimuli as our patients (rightmost panels in Fig. 5A and B). As can be seen, the range of fixational saccade amplitudes in subjects ZH and FC8 was smaller than in our patients when the latter reported seeing a stimulus. However, the shapes of the amplitude distributions were similar across patients and controls. In fact, subject CH exhibited larger fixational saccades than the other two controls, and the amplitudes of this subject's fixational saccades quantitatively overlapped with the patients' eye movements. To illustrate this, the inset of the rightmost panel of Fig. 5B shows the amplitude distribution of this subject's fixational saccades along with the amplitude distribution of patient TU-21 when this patient reported seeing the stimulus. In this inset, we normalized the distribution curves to demonstrate how similar these curves looked in the patient and the control. Thus, even though 2 of the 3 controls had better fixational stability than our patients, the distributions of saccade amplitudes were similar, and the amplitudes of patient TU-21 and control subject CH exhibited a large amount of overlap.

3.4. The efficacy of implant stimulation frequency could be related to saccade and microsaccade timing

Having identified oculomotor events (saccades versus ocular drifts) that occurred with and without visibility reports, we next turned our attention to analyzing possible oculomotor factors influencing how well patients could see with the subretinal implant.

As described earlier, 5 Hz retinal stimulation resulted in longer visibility durations than 2 Hz stimulation. The presence of eye movements could be one reason for this phenomenon. 2 Hz stimulation effectively causes stroboscopic stimuli. With 5 Hz stimulation, it would be easier to stabilize gaze because a sample is presented more often. Thus, oculomotor behavior in relation to retinal stimulation frequency will matter for percept onset and maintenance.

Additionally, 2 Hz stimulation might be expected to modify microsaccade and saccade timing beyond the normal operating range, since visual flicker is known to entrain the saccadic system (Hafed & Ignashchenkova, 2013; West & Boyce, 1968). For example, 2 Hz visual flicker would be expected to result in inter-saccadic intervals of ~500 ms, which is longer than the normal average of ~250–300 ms. We confirmed this by analyzing inter-saccadic intervals in two control subjects who fixated a stimulus flickering at either 2 or 5 Hz (Section 2). The inter-saccadic intervals from one of these subjects (ZH) are shown in Fig. 6A and B. 2 Hz visual flicker resulted in a peak of inter-saccadic intervals at ~500 ms and additional peaks at ~1000 and ~1500 ms consistent with entrainment (Hafed & Ignashchenkova, 2013; West & Boyce, 1968). For 5 Hz visual flicker, when saccades occurred, this subject's inter-saccadic intervals were closer to 200–250 ms, and the distribution was unimodal (Fig. 6B). The distribution of inter-saccadic intervals in our patients with 5 Hz retinal stimulation was also unimodal (Fig. 6C and D). For patient TU-21, the median interval was 406.5 ms, and it was 363 ms for patient TU-09, both less than 500 ms. Moreover, the peaks in the distributions were also both less than 500 ms, which would be the expected peak at 2 Hz stimulation. Thus, 5 Hz visual flicker in controls resulted in unimodal inter-saccadic interval distributions that were qualitatively similar to those of the patients, providing a possible reason for why 5 Hz retinal stimulation could result in longer visibility intervals. Note that we could not repeat the analysis of Fig. 6A for patient TU-09 when he was run at 2 Hz retinal stimulation, because this patient's visibility durations were too brief in this condition to allow us to measure inter-saccadic intervals as large as 500 or 1000 ms.

3.5. Both ocular drifts and microsaccades/saccades contributed to the gaining and losing of visibility

Beyond inter-saccadic intervals, we found that, even with 5 Hz stimulation, ocular drift, saccades, and microsaccades could still

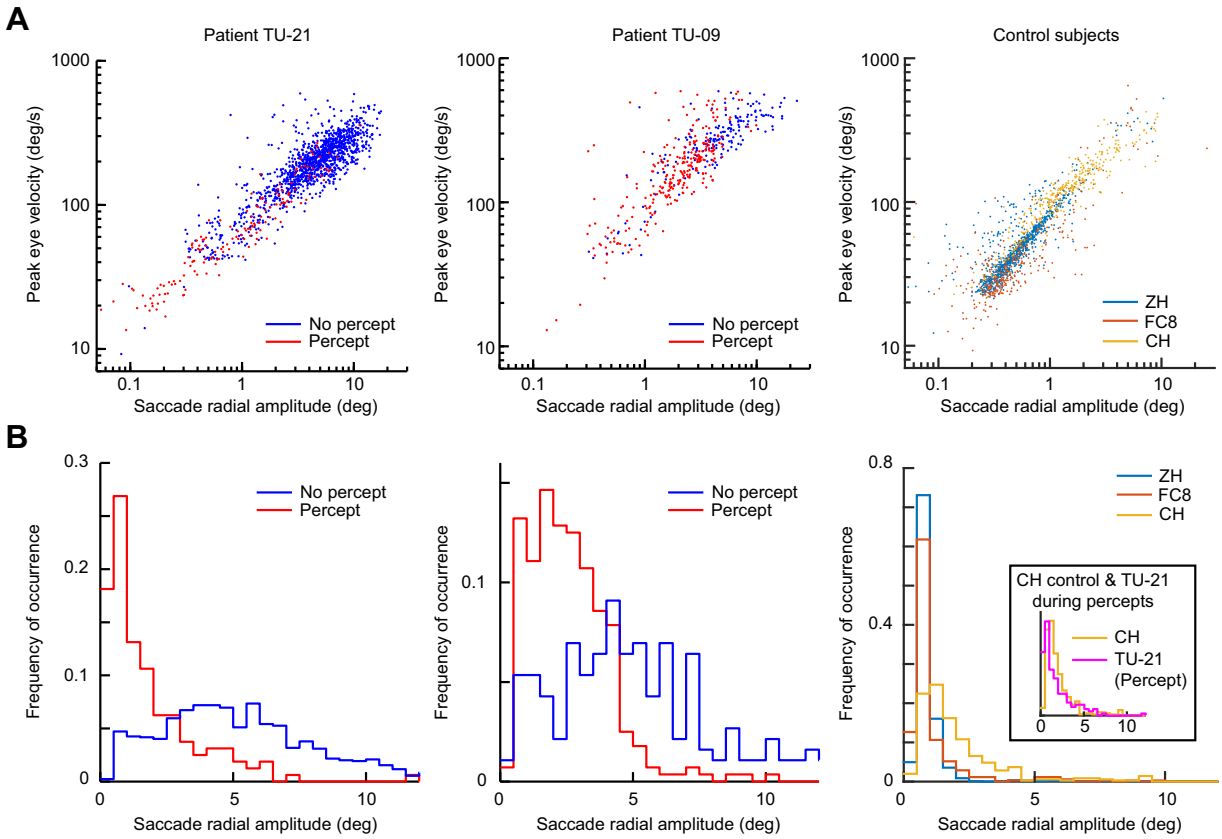

Fig. 5. Saccade distributions reflected the patients' percepts and their stability of fixation during such percepts. (A) The main sequence relationship between saccade peak velocity and saccade radial amplitude for the two patients (left two panels) and the three controls (rightmost panel). Each dot represents a saccade, and the different colors in the patient panels indicate whether the saccade occurred when the subject was reporting a stimulus percept (red) or not (blue). Different colors in the control panel indicate the different control subjects. Saccades in the patients fell on a "main sequence" relationship (Zuber et al., 1965), and the eye movements were significantly smaller when a patient reported seeing a stimulus than when he reported invisibility. (B) Distributions of saccade amplitudes in the two patients with and without a stimulus percept (left two panels) and in the three controls (rightmost panel). Consistent with A, eye movements in the patients were smaller during visibility intervals than during invisibility intervals. The inset in the rightmost panel compares the amplitude distribution of control subject CH to that of patient TU-21 (after normalizing each curve to facilitate comparing the shapes of the two distributions). As can be seen, there was a large amount of overlap between the two individuals, and the shapes of the amplitude distributions were also similar.

influence the maintenance or loss of stimulus visibility in our patients.

In terms of ocular drift, we found that the gaining and losing of a stimulus can sometimes be entirely attributed to changes in eye position. To illustrate this, Fig. 7A shows eye position from a sample trial of the localization task in patient TU-21. The patient experienced two visibility intervals separated by one interval without visibility. Closer inspection of the figure revealed a clear vertical drift of the eye during both periods of visibility. Specifically, the subject first found the stimulus when eye position was at a specific location and lost the percept when eye position drift prevented the visual field of the implant (<∼10–15° of central visual field) from "seeing" the stimulus. In both visibility intervals, eye position at either the beginning or end of the percept was similar, and the trajectory of the eye during each interval was also similar (as illustrated in Fig. 7B with the eye data in both visibility intervals overlaid on top of each other). This remarkable repeatability happened despite the passage of many intervening seconds, and many intervening blinks and saccades, in the time span between the two visibility reports. Moreover, this repeatability was also visible when we plotted the two-dimensional scanpath trajectory of the eye during the two visibility intervals (Fig. 7C; also see Supplementary Movie S1). As can be seen, the two trajectories started at similar physical eye positions, moved similarly with downward drift, and ended at similar physical eye positions (save for a horizontal saccade in the first visibility interval that likely contributed to the loss of visibility at the end of that interval). Thus, ocular drift over the stimulus could significantly influence visibility for implant patients.

The second way that oculomotor behavior could be correlated with visibility reports is through the use of saccades and microsaccades. These eye movements cause neural excitability in retina (Amthor, Tootle, & Gawne, 2005; Segev et al., 2007), LGN (Reppas, Usrey, & Reid, 2002), and primary visual cortex (Kagan et al., 2008; Martinez-Conde, Macknik, & Hubel, 2000; Rajkai et al., 2008) after they occur. This excitability is very likely due to "refreshing" of retinal images (Amthor et al., 2005; Segev et al., 2007). If this is the case, then it may be possible that our patients sometimes transitioned from periods of visibility to periods of invisibility when saccade frequency decreased during prolonged fixation. To investigate this hypothesis, we analyzed data from the 5 Hz stimulation sessions in both patients. We analyzed all percepts lasting for longer than 1 s, and we measured the average number of saccades/microsaccades that occurred in the first second of a percept (i.e. after transitioning from invisibility to visibility). We then compared this number to the average number of saccades/microsaccades that occurred in the final second of a percept (we defined the final second of the percept as the second ending −200 ms relative to the button release by the patients, in order to account for an approximate manual reaction time after the

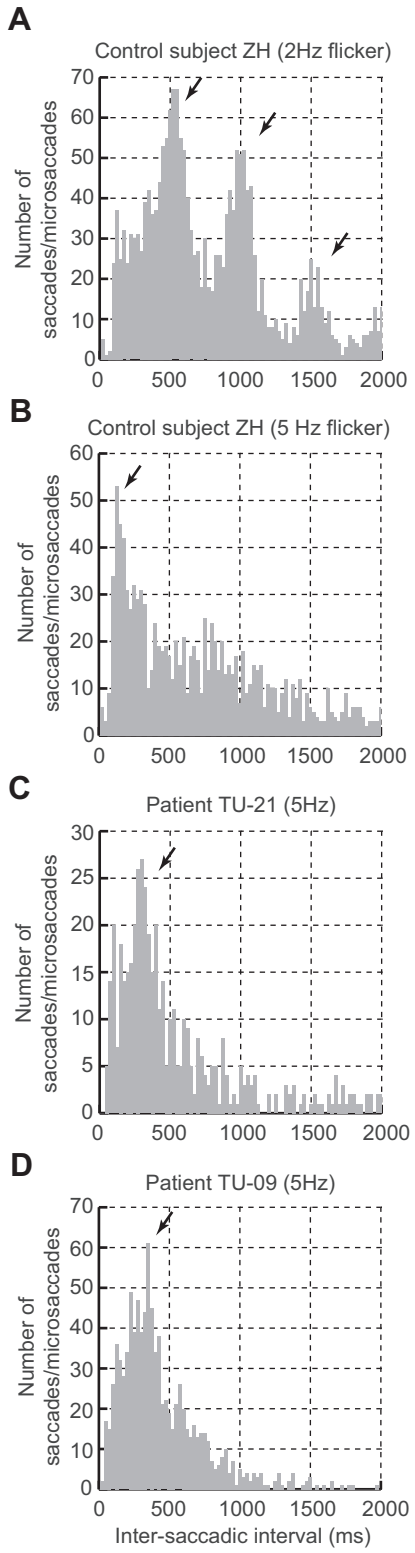

Fig. 6. Saccade/microsaccade timing could be influenced by visual or retinal stimulation frequency. (A, B) We tested control subjects with visual stimuli flickering at 2 Hz (A) or 5 Hz (B) to simulate the retinal implant patients' stimulation regimes. Saccades and microsaccades entrained to the visual flicker frequency such that inter-saccadic intervals at 2 Hz were ~500 ms and multiples thereof, whereas they were ~200–250 ms and with a unimodal distribution at 5 Hz. This latter value is close to normal inter-saccadic intervals with steady visual stimulation. (C, D) The patients showed similar unimodal inter-saccadic interval distributions to the controls when their implants were run at 5 Hz.

actual loss of the stimulus). Close to the end of a visibility report, patient TU-21 was making significantly less saccades/microsaccades than at the beginning ($p < 0.05$; t-test, Fig. 8), suggesting that eye movements could potentially contribute to the refreshing of retinal images, and thus percept durations, in patients with a subretinal implant. For the second patient (TU-09), the difference in the same analysis was not significant (likely due to nystagmus), but the trend was in the same direction.

Thus, the analyses of Figs. 7 and 8 combined suggest that both ocular drift and saccades/microsaccades exhibited correlations with the onsets and offsets of visibility reports by our patients. This information may be used to develop oculomotor training strategies for the patients in order to improve their utilization of their implants.

3.6. Eye tracking provided an objective measure of implant performance beyond subjective reports by the patients

Finally, we asked whether eye movements could be used as an objective tool for evaluating retinal implant performance beyond subjective report, as patients may sometimes be hesitant about their perceptual answers. To investigate this possibility, we analyzed the distribution of saccade metrics during our shapes task, and we asked whether the specific geometry of a shape that patients were looking at could influence their eye movements.

In general, the patients were not accurate in their perceptual reports of the shapes. This could be due to several factors, including hesitancy by the patients themselves as well as their limited spatial acuity. However, when we analyzed their saccades, we found that the distributions of these saccades were influenced by shape properties, consistent with a known role of eye movements in scanning visual objects (Moore, 1999; Yarbus, 1967). We calculated the proportion of predominantly horizontal saccades – saccades whose horizontal amplitude was larger than their vertical amplitude – observed when the patients reported seeing an object, and we compared this proportion across the different shapes. For example, we reasoned that the horizontal rectangle would recruit more predominantly horizontal saccades than the square, by virtue of its shape.

We found that different shapes altered the distributions of generated saccades when the patients saw the stimulus. To illustrate this, Fig. 9A–C shows an example of this effect for the case of square versus rectangle (Fig. 9A for a control subject and Fig. 9B for both of our patients combined, but only from the periods in which they reported seeing a stimulus). Like the control, patients exhibited more predominantly horizontal saccades when they were scanning a horizontal rectangle rather than a square. Individually, the difference in patient TU-21 was statistically significant at the $p < 0.05$ level (using a Z-test on the hypothesis that square had less horizontal saccades than the rectangle). For the second patient (TU-09), the same trend was present, but it did not reach this significance level (p-value: 0.065), and that is why we combined data from both patients in this analysis. Importantly, in both patients, this effect was gone when we repeated the same analysis during invisibility intervals (Fig. 9C). This indicates that shapes influenced eye movement metrics when the patients saw these shapes through their implants.

Fig. 9E shows saccade amplitudes during visibility periods; because the rectangle was physically smaller than the square, saccade amplitudes in the rectangle were smaller. When the patients could not see the stimulus (Fig. 9F), the same analysis showed a much smaller difference in saccade amplitudes across the two conditions. Note that controls in this condition showed smaller eye

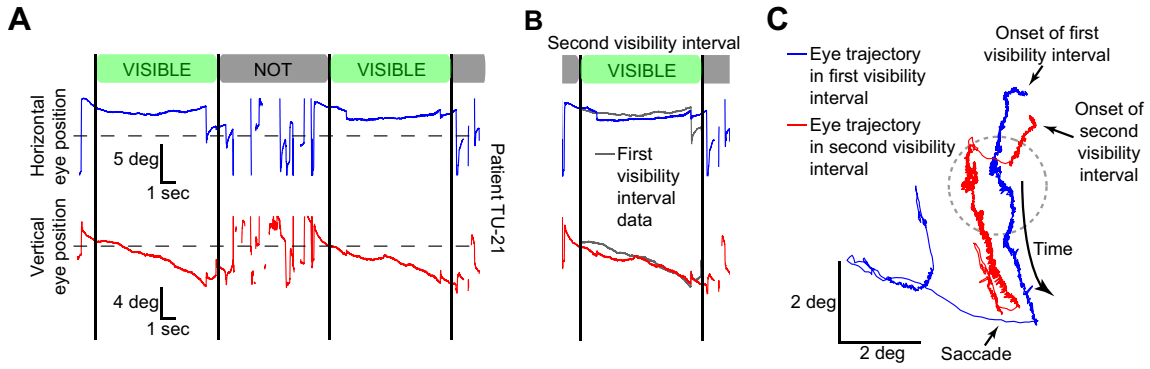

Fig. 7. Ocular position and drift contributed to the onsets and offsets of percepts. (A) Eye position data in a format qualitatively similar to that in Fig. 2. Here, we show a trial with two intervals of visibility separated by several seconds without. In both visibility intervals, eye position showed very similar trajectories. This indicates that eye movements are repeatable for a given stimulus, which is consistent with the conclusions of Fig. 4. (B) In this panel, we overlaid eye positions from both visibility intervals on top of each other. The second visibility interval started when eye position landed at a similar position to when the first visibility interval started, and it ended after the eye had drifted to a position that was similar to the position when the first interval ended (except for a saccade at the end of the first visibility interval, which likely contributed to the loss of the percept in that interval). (C) Two-dimensional eye position trajectories for the two visibility intervals in (A, B). In both intervals, percept onset and percept offset occurred at very specific eye positions, which presumably brought the implant onto or away from the visual stimulus. We show the size of the stimulus that the patient was trying to fixate to provide a reference for how large the drift needed to be before the stimulus was lost. The range of drift that the subject exhibited before losing the percept was of a magnitude consistent with this patient's visual field afforded by the implant. Also see Supplementary Movie S1.

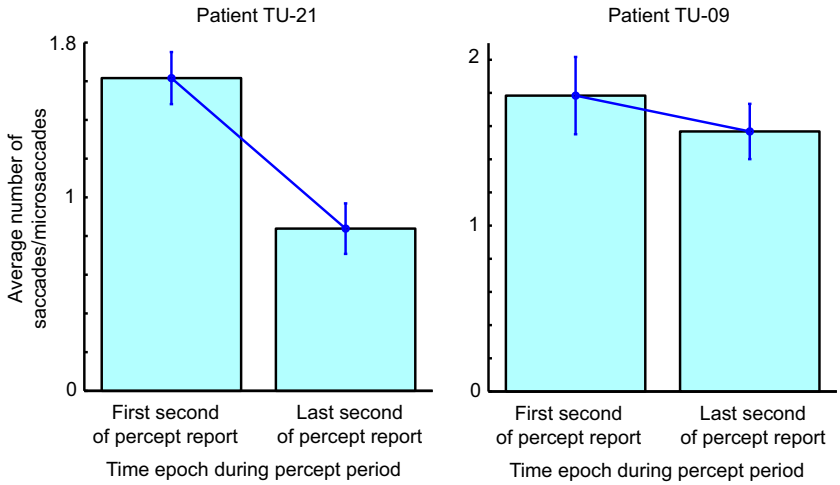

Fig. 8. Saccade/microsaccade frequencies at the ends of visibility intervals were lower than at the beginnings of these intervals. For each patient, we plotted the average number of saccades/microsaccades that occurred in the first second of visibility reports and compared it to the average number of saccades/microsaccades that occurred in the final second of visibility reports. In both patients, the latter number was lower than the former number. Error bars denote s.e.m.

movements than the patients. This could be due to nystagmus in the patients' eyes (e.g. Fig. 2C).

4. Discussion

We characterized oculomotor behavior of blind patients seeing with a subretinal electronic implant. We found that eye movements reliably reflected perception, and that they provided an objective measure of stimulus location. Importantly, the patients' scanning and fixational eye movements were qualitatively similar to controls. We also observed an influence of stimulus shape on the patients' eye movements, despite uncertainty by the patients themselves on what shapes they saw. This suggests that eye movements can act as an important objective diagnostic tool for evaluating the success of retinal implants. Finally, both ocular drifts and saccades/microsaccades during stimulus visibility intervals could contribute to either maintaining such visibility or losing it. Specifically, drifts could move the implant photodetector array away from or towards the stimulus location, and a decreased saccade/microsaccade frequency was correlated with the end of visibility.

Our results indicate that ocular drifts and microsaccades have an important role in artificial vision with electronic implants. We observed in our patients both smooth drifts as well as microsaccades, with the latter occurring either singly or as "square-wave" couplets (Fig. 3). This is an interesting observation because fixational eye movements serve an important function for retinal processing. These eye movements alter the position of retinal tissue that is being stimulated by the subretinal electrodes, without shifting gaze away from the object that is being viewed. Moreover, these different types of eye movements have been implicated in different perceptual processing phenomena. For example, microsaccades/saccades refresh retinal images, causing strong transients in retina and beyond (Amthor et al., 2005; Kagan et al., 2008; Martinez-Conde et al., 2000; Reppas et al., 2002; Segev et al., 2007). Ocular drifts (besides also moving retinal images, although without as strong transients) may modulate image statistics to support perception (Kagan & Hafed, 2013; Kuang et al., 2012; Poletti et al., 2013). This is in addition to the potential

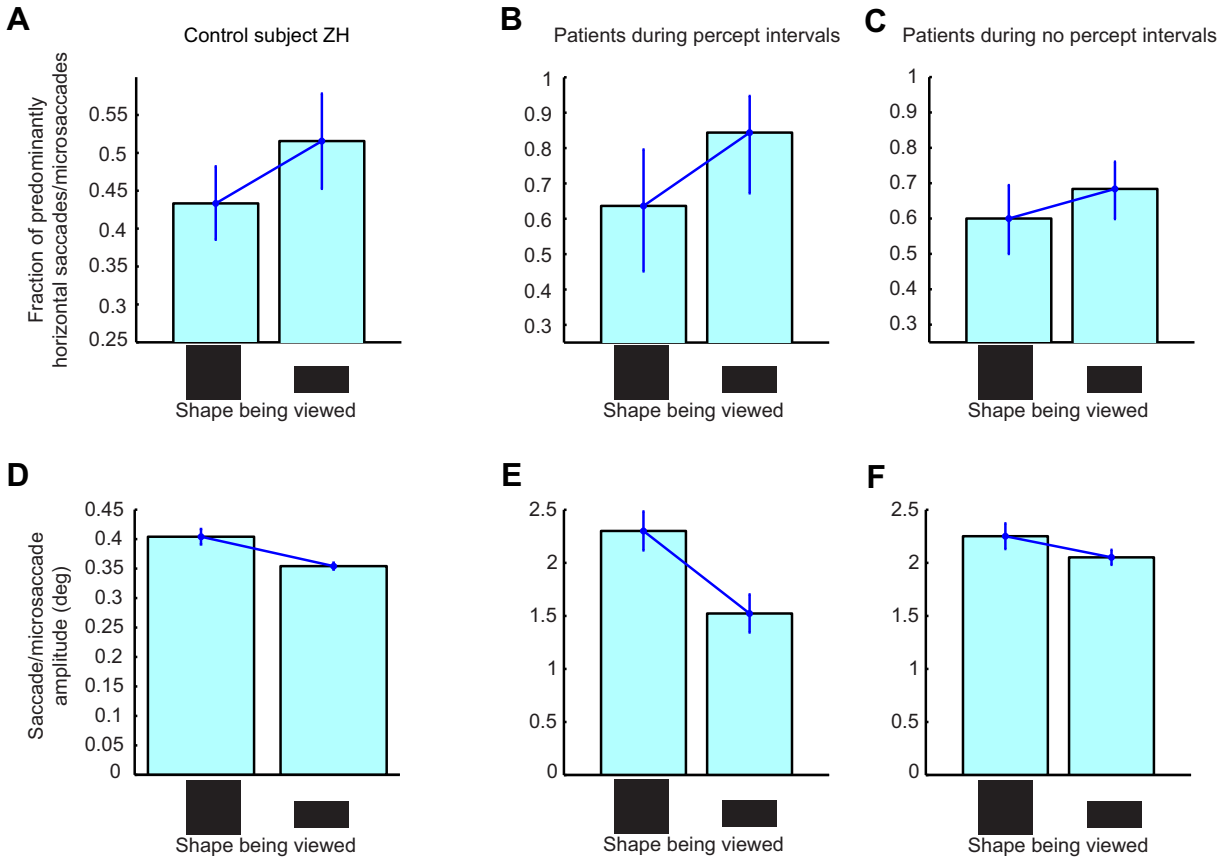

Fig. 9. Viewed shapes influenced eye movement metrics when visibility was reported but not as much when no visibility was reported. (A–C) Proportion of all saccades/microsaccades that were predominantly horizontal as a function of whether subjects were looking at a square or a horizontal rectangle. When visibility was reported (B), the rectangle had more horizontal saccades/microsaccades, consistent with control subjects (A). This was not the case when visibility was not reported (C), indicating that stimulus visibility mattered. (D–F) Similar analyses for saccade/microsaccade amplitudes. When a stimulus was seen by the patients (E), the eye movements used to look at the stimulus were smaller for the smaller shape. This effect was much less obvious when the stimulus was invisible (F).

involvement of fixational eye movements in cognitive processes like attention beyond just retinal image modulation (Engbert & Kliegl, 2003; Hafed, 2013; Hafed & Clark, 2002; Pastukhov & Braun, 2010; Pastukhov et al., 2012). Thus, the presence of fixational and non-fixational eye movements in our patients provides strong support for the use of light sensitive subretinal implants, as they can harness the full power of ocular motility in the patients.

Our observation of decreased saccadic activity towards the ends of visibility reports might suggest that the "refreshing" role of microsaccades and saccades on retinal images may help in the sustenance of percepts by retinal implants, such as in natural vision. Alternatively, or perhaps additionally, it could also be the case that fatigue during fixation may result in a loss of attention or arousal in the fixation task. Such loss may in turn reduce the efficacy of active oculomotor control over corrective eye movements, which could cause the eye to deviate away from the stimulus and result in lost visibility. Either way, our results suggest how eye movements can be related to artificial vision with electronic retinal implants.

Our patients were naïve to the purposes of the study, and they had only been using their implants for a few weeks or months prior. Thus, their oculomotor behavior was very natural. Eye tracking could therefore be a useful and non-invasive way for clinical evaluation of retinal implant patients, as well as a training tool. In fact, even with minimal training, the localization task allowed us to establish that eye movements can be specific to stimuli and also allowed us to obtain approximate calibration resolution estimates to check the size of fixational saccades. The fact that the eye did better than the patient report in the shapes task also suggests that eye tracking might be an important objective diagnostic tool. This observation is itself intriguing, but it might be due to slightly different pathways mediating conscious perceptual interpretation of shapes and eye movement control. It is also reminiscent of observations in which some subjects can perform better than they feel in a variety of psychophysical scenarios.

We found that higher stimulation frequency can lead to a higher quality of perception in our patients. In particular, visibility durations with 2 Hz stimulation were shorter that those with 5 Hz stimulation. There could be several reasons for variable percept durations, including biochemical adaptations to repeated electrical stimulation of neural tissue. However, we hypothesized that oculomotor behavior could be an additional contributor to such changes in visibility. After all, the patients are looking at the world through a limited visual field of about 10–15° provided by their implants, and if they moved their eyes such that the subretinal array did not "see" or has lost the stimulus in between the stimulation intervals, they would be expected to lose the percept. Given this fact, it might be understandable why 2 Hz stimulation was more challenging than 5 Hz stimulation. 2 Hz stimulation is stroboscopic. So, if the eye is moving, a flash may be long gone after an eye movement. In fact, our patients often reported that when they were searching for the stimulus, they sometimes saw it "zoom by" but had a hard time remembering how to go back to it after they realized that they saw it. With 5 Hz stimulation, this is less of a problem because a sample is presented to the eye every 200 ms.

Our simulated results with 2 Hz flicker also highlight additional potential reasons for why implant technologies can benefit from higher stimulation rates: subjectively, the 2 Hz condition was not as comfortable as the 5 Hz condition for our controls. Importantly, the flicker with 2 Hz seemed to additionally cause shape distortions such that the flickering circle sometimes appeared to the controls as having straight edges like a hexagon. This could potentially explain some of the difficulty in shape discrimination experienced by our patients.

The calibration that we were able to obtain with the localization task was challenging for our analyses, for several reasons. Not only was the geometry of eye tracking unusual, but the patients were also not experts in our laboratory environment. They may have fidgeted during the session, and squinted their eyes, resulting in some increased variability in eye calibration compared to well-trained expert control subjects. Additionally, we measured a blind, non-dominant, and often strabismic eye. This eye sometimes even had nystagmus, as was particularly prominent in patient TU-09. All of these factors may have increased variability in our eye calibration results compared to controls (e.g. Fig. 4). However, despite all of these challenges, our present results still represent a step forward in integrating oculomotor studies with retinal implant evaluations. Looking ahead, beyond tackling this challenge and those we highlighted throughout this paper, there exist many new interesting questions that now arise, and that are ripe for future investigations.

One such investigation could attempt to elucidate the role of eye movements in perceptual stability in our patients. Specifically, the stimulus conditions that our patients experienced in our study are ones that increase the chance of classic perceptual illusions of motion, like autokinesis (Poletti, Listorti, & Rucci, 2010; Verheijen & Oosting, 1964). In this illusion, a stationary object seen in complete darkness will soon be experienced to move continuously. Some of our control subjects did experience this illusion in their sessions, as did the patients. Moreover, the drifts we saw in Fig. 7 are reminiscent of what might happen if images were retinally stabilized with no additional reference frames to stabilize gaze. The lack of references may result in the eye wandering away, because this is a property of the oculomotor control system. All of these factors might contribute to illusions of motion, and it would be interesting to understand them more.

5. Conclusions

We measured eye movements in blind patients seeing with a subretinal electronic implant. When the patients saw stimuli through their implants, they fixated very well, and their fixational eye movements were qualitatively similar to those of controls even with little training. Our analyses of eye movements allowed us to identify possible oculomotor factors influencing perception quality and duration, and these analyses suggest that eye tracking is an extremely useful objective tool for evaluating the function of visual implants.

Conflicts of interest

ZH, KB, and FG report no conflicts of interest.

KS is employed by the University of Tuebingen through financial support from Retina Implant AG, Reutlingen, Germany for the clinical trial, and she received travel support.

EZ owns stock in Retina Implant AG, Reutlingen, Germany. He is also a paid consultant, holder of patents as inventor/developer, and recipient of travel support from Retina Implant AG, Reutlingen, Germany.

Acknowledgments

ZMH and EZ were supported by the Werner Reichardt Centre for Integrative Neuroscience at the Eberhard Karls University of Tuebingen. The Centre for Integrative Neuroscience is an Excellence Cluster funded by the Deutsche Forschungsgemeinschaft (DFG) within the framework of the Excellence Initiative (EXC 307). This work was also supported by Retina Implant AG, Reutlingen, Germany, and it is also part of the research programme of the Bernstein Center for Computational Neuroscience, Tübingen, funded by the German Federal Ministry of Education and Research (BMBF; FKZ: 01GQ1002).

The authors thank the following staff of Retina Implant AG, Reutlingen, Germany: Walter Wrobel, Udo Greppmaier, Maren Malcherzyk, and Angelika Braun.

Appendix A. Supplementary data

Supplementary data associated with this article can be found, in the online version, at http://dx.doi.org/10.1016/j.visres.2015.04.006.

References

Abadi, R. V., Scallan, C. J., & Clement, R. A. (2000). The characteristics of dynamic overshoots in square-wave jerks, and in congenital and manifest latent nystagmus. *Vision Research, 40*, 2813–2829.

Amthor, F. R., Tootle, J. S., & Gawne, T. J. (2005). Retinal ganglion cell coding in simulated active vision. *Visual Neuroscience, 22*, 789–806.

Chen, C. Y., & Hafed, Z. M. (2013). Postmicrosaccadic enhancement of slow eye movements. *Journal of Neuroscience, 33*, 5375–5386.

Coppola, D., & Purves, D. (1996). The extraordinarily rapid disappearance of entopic images. *Proceedings of the National Academy of Sciences of the United States of America, 93*, 8001–8004.

Eickenscheidt, M., Jenkner, M., Thewes, R., Fromherz, P., & Zeck, G. (2012). Electrical stimulation of retinal neurons in epiretinal and subretinal configuration using a multicapacitor array. *Journal of Neurophysiology, 107*, 2742–2755.

Engbert, R., & Kliegl, R. (2003). Microsaccades uncover the orientation of covert attention. *Vision Research, 43*, 1035–1045.

Feldon, S. E., & Langston, J. W. (1977). Square-wave jerks: A disorder of microsaccades? *Neurology, 27*, 278–281.

Hafed, Z. M. (2013). Alteration of visual perception prior to microsaccades. *Neuron, 77*, 775–786.

Hafed, Z. M., & Clark, J. J. (2002). Microsaccades as an overt measure of covert attention shifts. *Vision Research, 42*, 2533–2545.

Hafed, Z. M., & Krauzlis, R. J. (2010). Microsaccadic suppression of visual bursts in the primate superior colliculus. *Journal of Neuroscience, 30*, 9542–9547.

Hafed, Z. M., & Ignashchenkova, A. (2013). On the dissociation between microsaccade rate and direction after peripheral cues: Microsaccadic inhibition revisited. *Journal of Neuroscience, 33*, 16220–16235.

Hafed, Z. M., Goffart, L., & Krauzlis, R. J. (2009). A neural mechanism for microsaccade generation in the primate superior colliculus. *Science, 323*, 940–943.

Humayun, M. S., Dorn, J. D., da Cruz, L., Dagnelie, G., Sahel, J. A., Stanga, P. E., et al. (2012). Interim results from the international trial of Second Sight's visual prosthesis. *Ophthalmology, 119*, 779–788.

Kagan, I., & Hafed, Z. M. (2013). Active vision: Microsaccades direct the eye to where it matters most. *Current Biology, 23*, R712–714.

Kagan, I., Gur, M., & Snodderly, D. M. (2008). Saccades and drifts differentially modulate neuronal activity in V1: Effects of retinal image motion, position, and extraretinal influences. *Journal of Vision, 8*(19), 11–25.

Ko, H. K., Poletti, M., & Rucci, M. (2010). Microsaccades precisely relocate gaze in a high visual acuity task. *Nature Neuroscience, 13*, 1549–1553.

Krauzlis, R. J., & Miles, F. A. (1996). Release of fixation for pursuit and saccades in humans: Evidence for shared inputs acting on different neural substrates. *Journal of Neurophysiology, 76*, 2822–2833.

Kuang, X., Poletti, M., Victor, J. D., & Rucci, M. (2012). Temporal encoding of spatial information during active visual fixation. *Current Biology, 22*, 510–514.

Leopold, D. A., & Logothetis, N. K. (1998). Microsaccades differentially modulate neural activity in the striate and extrastriate visual cortex. *Experimental Brain Research, 123*, 341–345.

Martinez-Conde, S., Macknik, S. L., & Hubel, D. H. (2000). Microsaccadic eye movements and firing of single cells in the striate cortex of macaque monkeys. *Nature Neuroscience, 3*, 251–258.

Moore, T. (1999). Shape representations and visual guidance of saccadic eye movements. *Science, 285*, 1914–1917.

Pastukhov, A., & Braun, J. (2010). Rare but precious: Microsaccades are highly informative about attentional allocation. *Vision Research, 50*, 1173–1184.

Pastukhov, A., Vonau, V., Stonkute, S., & Braun, J. (2012). Spatial and temporal attention revealed by microsaccades. *Vision Research, 85*, 45–57.
Perez Fornos, A., Sommerhalder, J., da Cruz, L., Sahel, J. A., Mohand-Said, S., Hafezi, F., et al. (2012). Temporal properties of visual perception on electrical stimulation of the retina. *Investigative Ophthalmology and Visual Science, 53*, 2720–2731.
Poletti, M., Listorti, C., & Rucci, M. (2010). Stability of the visual world during eye drift. *Journal of Neuroscience, 30*, 11143–11150.
Poletti, M., Listorti, C., & Rucci, M. (2013). Microscopic eye movements compensate for nonhomogeneous vision within the fovea. *Current Biology, 23*, 1691–1695.
Rajkai, C., Lakatos, P., Chen, C. M., Pincze, Z., Karmos, G., & Schroeder, C. E. (2008). Transient cortical excitation at the onset of visual fixation. *Cerebral Cortex, 18*, 200–209.
Reppas, J. B., Usrey, W. M., & Reid, R. C. (2002). Saccadic eye movements modulate visual responses in the lateral geniculate nucleus. *Neuron, 35*, 961–974.
Riggs, L. A., Ratliff, F., Cornsweet, J. C., & Cornsweet, T. N. (1953). The disappearance of steadily fixated visual test objects. *Journal of the Optical Society of America, 43*, 495–501.
Segev, R., Schneidman, E., Goodhouse, J., & Berry, M. J. 2nd, (2007). Role of eye movements in the retinal code for a size discrimination task. *Journal of Neurophysiology, 98*, 1380–1391.
Stampe, D. M. (1993). Heuristic filtering and reliable calibration methods for video-based pupil-tracking systems. *Behavior Research Methods, Instruments, & Computers, 25*, 137–142.
Stingl, K., Bartz-Schmidt, K. U., Gekeler, F., Kusnyerik, A., Sachs, H., & Zrenner, E. (2013). Functional outcome in subretinal electronic implants depends on foveal eccentricity. *Investigative Ophthalmology & Visual Science, 54*, 7658–7665.
Stingl, K., Bartz-Schmidt, K. U., Besch, D., Braun, A., Bruckmann, A., Gekeler, F., et al. (2013). Artificial vision with wirelessly powered subretinal electronic implant alpha-IMS. *Proceedings of the Royal Society B: Biological Sciences, 280*, 20130077.
Verheijen, F. J., & Oosting, H. (1964). Mechanism of visual autokinesis. *Nature, 202*, 979–981.
West, D. C., & Boyce, P. R. (1968). The effect of flicker on eye movement. *Vision Research, 8*, 171–192.
Yarbus, A. L. (1967). *Eye movements and vision*. New York: Plenum Press.
Zrenner, E. (2002). Will retinal implants restore vision? *Science, 295*, 1022–1025.
Zrenner, E. (2013). Fighting blindness with microelectronics. *Science Translational Medicine, 5*, 210ps216.
Zrenner, E., Bartz-Schmidt, K. U., Benav, H., Besch, D., Bruckmann, A., Gabel, V. P., et al. (2011). Subretinal electronic chips allow blind patients to read letters and combine them to words. *Proceedings of the Royal Society B: Biological Sciences, 278*, 1489–1497.
Zuber, B. L., Stark, L., & Cook, G. (1965). Microsaccades and the velocity–amplitude relationship for saccadic eye movements. *Science, 150*, 1459–1460.